

INFORMATION TO USERS

This manuscript has been reproduced from the microfilm master. UMI films the text directly from the original or copy submitted. Thus, some thesis and dissertation copies are in typewriter face, while others may be from any type of computer printer.

The quality of this reproduction is dependent upon the quality of the copy submitted. Broken or indistinct print, colored or poor quality illustrations and photographs, print bleedthrough, substandard margins, and improper alignment can adversely affect reproduction.

In the unlikely event that the author did not send UMI a complete manuscript and there are missing pages, these will be noted. Also, if unauthorized copyright material had to be removed, a note will indicate the deletion.

Oversize materials (e.g., maps, drawings, charts) are reproduced by sectioning the original, beginning at the upper left-hand corner and continuing from left to right in equal sections with small overlaps. Each original is also photographed in one exposure and is included in reduced form at the back of the book.

Photographs included in the original manuscript have been reproduced xerographically in this copy. Higher quality 6" x 9" black and white photographic prints are available for any photographs or illustrations appearing in this copy for an additional charge. Contact UMI directly to order.

UMI

A Bell & Howell Information Company
300 North Zeeb Road, Ann Arbor MI 48106-1346 USA
313/761-4700 800/521-0600

RICE UNIVERSITY

**Noble Gas Endohedral Complexes
of C₆₀ Buckminsterfullerene**

by

Richard Darzynkiewicz

A THESIS SUBMITTED
IN PARTIAL FULFILLMENT OF THE
REQUIREMENTS FOR THE DEGREE

Master of Arts

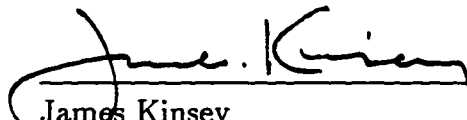
APPROVED, THESIS COMMITTEE:



Gustavo Scuseria, Chairman
Professor of Chemistry



Philip Brooks
Professor of Chemistry



James Kinsey
Professor of Chemistry

Houston Texas

May, 1997

UMI Number: 1384352

UMI Microform 1384352
Copyright 1997, by UMI Company. All rights reserved.

**This microform edition is protected against unauthorized
copying under Title 17, United States Code.**

UMI
300 North Zeeb Road
Ann Arbor, MI 48103

Abstract

Noble Gas Endohedral Complexes of C₆₀ Buckminsterfullerene

by

Richard Darzynkiewicz

Equilibrium geometries and binding energies (corrected for basis set superposition error) of single and multiple noble gas atom complexes of C₆₀ are calculated at DFT and MP2 levels of theory using basis sets including polarization functions. B3LYP and MP2 give similar van der Waals dispersion interactions, predicting repulsive energies for the He and Ne complexes of about 1 kcal/mol, and higher energies for the larger noble gas atom complexes. As expected, C₆₀ is resilient to deformation in all cases studied, with the geometry of the fullerene cage barely affected by the presence of multiple noble gas atoms inside.

Acknowledgments

Dr. Gustavo Scuseria is acknowledged for his patient guidance.

Friends and family are acknowledged for their support.

Thanks everyone!

Table of Contents

| | |
|----------------------------------|----|
| Chapter 1: Introduction | 1 |
| Chapter 2: Computational Details | 6 |
| Chapter 3: Results | 11 |
| Chapter 4: Conclusions | 21 |
| References | 23 |

List of Figures

| | | |
|-----------|--|----|
| Figure 1. | van der Waals based space filling depictions | 5 |
| Figure 2. | Two views of four isomers of $\text{He}_2@C_{60}$ | 9 |
| Figure 3. | Three views of four isomers of $\text{He}_3@C_{60}$ and $\text{He}_4@C_{60}$ | 10 |

List of Tables

| | | |
|----------|---|----|
| Table 1. | Optimized radii and bond lengths | 14 |
| Table 2. | Optimized radii | 15 |
| Table 3. | Binding energies | 16 |
| Table 4. | Basis set superposition error corrected binding energies | 17 |
| Table 5. | C ₆₀ strains | 18 |
| Table 6. | Binding energies, basis set superposition error corrected binding energies, and C ₆₀ strains | 19 |
| Table 7. | Binding energies, basis set superposition error corrected binding energies, and C ₆₀ strains | 20 |

Chapter 1

Introduction

The discovery of fullerenes entailed graphite vaporization by a pulsed laser in a He atmosphere [1]. Inert gas was used both as a buffer and carrier gas, cooling the graphite and transporting carbon clusters to a mass spectrometer. Modifying the pressure of the He gas inside the apparatus changed the amount of buckminsterfullerene produced relative to other cluster species. Pressures of about one atmosphere of He over the graphite, with ample time of flight for cluster formation, were ideal conditions for C₆₀ formation. Currently, commercial C₆₀ formation via graphite vaporization is performed by arcing electric current between graphite electrodes in a He buffer gas of 0.2 atmospheres [2]. Although the exact pathway of fullerene formation from individual carbon atoms is unknown [3], when the cage finally closes, it may encapsulate one of the buffer gas atoms.

Bond lengths from gas phase electron diffraction experiments determine the radius of C₆₀ to be 3.562 Å [4, 5]. With carbon and He van der Waals atomic radii of 1.85 and 1.22 Å [6] respectively, there is room for the noble gas atom inside the fullerene without overlap of atomic radii. van der Waals based space filling depictions of single noble gas atom complexes of C₆₀ are shown in Figure 1. According to this hard sphere criterion, Ne can also fit inside C₆₀ without interaction, while Ar, Kr, and Xe have van der Waals overlap with the carbon atoms of the fullerene.

If one assumes that the concentration of the buffer gas is the same inside as outside the fullerene, the probability of the formation of a C_{60} fullerene encapsulating a He atom is the volume of the cavity times the concentration of He, about one per million fullerenes [7]. The expected probability decreases for Ne, with the prediction of zero incorporation in this way for Ar, Kr, and Xe.

Using a highly sensitive mass spectrometer [8], small amounts of noble gas atoms are detected from high temperature decomposition of samples containing these atoms. Fullerene commercially prepared by the carbon arc method of graphite vaporization was incrementally heated in this apparatus, and the amount of He released was measured at different temperatures [7]. It is believed that at lower temperatures, the He atoms detected were released from lattice sites outside the fullerenes, while at higher temperatures, the He is attributed to escape from inside of the fullerenes. About one in 880,000 fullerenes contained a He atom inside. The Arrhenius activation energy for this (first-order) process is calculated to be about 80 kcal/mol [7].

Incorporation of noble gas atoms into intact fullerenes is accomplished under high pressure, high temperature experimental conditions [9]. Decomposition experiments detect about one per 1000 fullerenes containing He, Ne, Ar, and Kr, and about one per 3500 fullerenes for Xe prepared in this way [10]. A more thorough examination of the release of noble gas atoms from fullerenes was done using $Ne@C_{60}$, where the rates of decomposition, and the subsequent escape of Ne were measured carefully. The activation energy required for the release of Ne from C_{60} based on reaction rates is calculated to be about 90 kcal/mol [11].

With pentagons and hexagons on the surface of C_{60} , the transition state geometry of the passage of a He atom through an intact fullerene can be approximated by cyclopentene or benzene, with a He atom inside the ring, on the plane of the molecule. Transition state energetics of He- C_5 structures have been shown to be larger than those with C_6 [12]. Transition state energies required for the passage of a He atom through benzene and graphitic $C_{24}H_{12}$ are on the order of 240 kcal/mol and 220 kcal/mol, respectively [13].

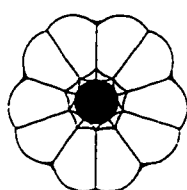
Experimental procedures which create noble gas atom- C_{60} complexes, and do not require the high pressure, high temperature conditions, include those entailing molecular beams [14]. Ion beams of fullerenes, aimed at stationary noble gas atoms, undergo collisions which force noble gas atoms, multiple noble gas atoms, and small diatomic molecules into fullerenes [15]. About 700 kcal/mol of energy is available in these collisions, more than twice what is calculated for the passage of noble gas atoms through six membered rings on the surface C_{60} .

To account for the relatively small energy barrier of release of noble gas atoms from C_{60} , a window mechanism is proposed [7]. A reversible breaking of a carbon-carbon bond on the surface of C_{60} is postulated to occur. One such window is a local minimum in the MNDO potential energy surface in the triplet state of C_{60} [16]. The energy required to create this window is roughly 70 kcal/mol above the triplet fullerene energy, and about 120 kcal/mol above the singlet energy. The transition state structure, with a He atom on the plane of the window, is calculated to be about 90 kcal/mol above the triplet state window minimum [17]. Energies of fullerenes with larger windows are within 100 kcal/mol of the ground state energy,

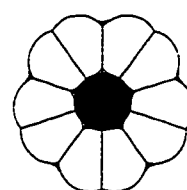
but He interaction raises the transition state barrier to above 200 kcal/mol for all windows studied.

Endohedral complexes with other atoms have also been created. It has been found that doping graphite with metals before vaporization leads to the formation of stable metallofullerenes [18], with one [19] or more [20, 21] metal atoms inside. Windows in fullerenes have also been chemically opened [22, 23], which could facilitate incorporation of small atoms inside. Possible uses for endohedral complexes of C_{60} range from the biological [24] to electrical [25]. The chemistry outside the fullerene has been examined [26], but the chemistry inside has not been fully probed without approximations in geometry [27] and systematic error correction [28]. Full geometry optimizations and accurate energy calculations with error corrections of single and multiple noble gas atom complexes with C_{60} are performed in this work, exploring the effects of the atoms inside on their buckminsterfullerene cage.

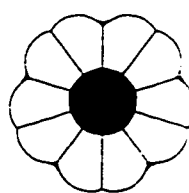
Figure 1
van der Waals^a based space filling depictions of X@C₆₀
(X = He, Ne, Ar, Kr, and Xe, radius of cavity^b = 1.71Å)



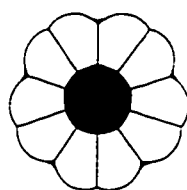
He@C₆₀



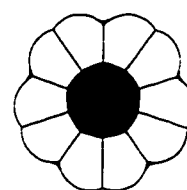
Ne@C₆₀



Ar@C₆₀



Kr@C₆₀



Xe@C₆₀

^a van der Waals radii are taken from ref [6]

^b C₆₀ radius is from ref [4, 5]

Chapter 2

Computational Details

The nomenclature used in this work to represent a noble gas atom inside a fullerene is $X@C_{60}$, where $X=He, Ne, Ar, Kr, \text{ and } Xe$. In the cases where more than one noble gas atom is inside C_{60} , the nomenclature is $X_n@C_{60}$, where $X=He \text{ and } Ne$, and $n=2, 3 \text{ and } 4$. Geometries with high degrees of symmetry are chosen to reduce the number of degrees of freedom in the calculations. In the cases of the single noble gas atom complexes with C_{60} , the icosahedral geometry is chosen. Icosahedral buckminsterfullerenes have two symmetry distinct bonds, which are referred here as 6-6 bonds and 5-6 bonds describing the bonds between two hexagons, and a hexagon and a pentagon on the surface of buckminsterfullerene, respectively. Multiple noble gas atom complex geometries are shown in Figures 2 and 3. $He_2@C_{60}$ configurations studied have the two noble gas atoms aligned along the axis bisecting hexagons, pentagons, 6-6 bonds, and 5-6 bonds, having D_{3d} , D_{5d} , C_{2h} , and D_{2h} symmetries, respectively. The only $Ne_2@C_{60}$ geometries studied are those with D_{3d} and D_{5d} symmetries because bond-open ring comparisons are made with $He_2@C_{60}$. $He_3@C_{60}$ complexes have He atoms arranged linearly along the D_{5d} and D_{3d} axis, and on a plane with C_{3v} and D_3 symmetries. The $He_4@C_{60}$ geometry chosen in this study is one with C_{3v} symmetry, with the noble gas atoms arranged in a pyramidal cluster inside the fullerene.

Geometry optimizations are carried out at two levels of density functional theory (DFT), with two different basis sets. The local spin density approximation [29], (LSDA) and Becke's three parameter exchange with Lee, Yang, and Parr's correlation [30] (B3LYP) are used with 3-21G and 6-31G** basis sets, except for calculations with Xe, where the 6-31G** basis set is not available. DFT methods have been shown to generate accurate geometries [31] and energies [32]. Single point DFT energy calculations of the optimized geometries are compared to the second order Moller-Plesset perturbation [33] (MP2) level of theory. A representative group of systems is chosen for B3LYP calculations with the larger basis set 6-311G**.

In this work, the binding energy (BE) is the energy of the reactants separately subtracted from the energy of the complex, $BE = E(X_n@C_{60}) - (nE(X) + E(C_{60}))$. BEs are systematically overestimated due to basis set superposition error (BSSE). BSSE correction is performed with counterpoise calculations [34]. The corrected binding energy (CBE) is the estimated BSSE subtracted from the BE. Comparisons between energies of the strained C_{60} in the configuration of the complex and of buckminsterfullerene at equilibrium are made to estimate the deformation of C_{60} caused by the noble gas atoms inside.

All calculations in this study are carried out using a developmental version of the GAUSSIAN [35] suite of programs. DFT applications entail a new weight scheme that has been shown to significantly decrease CPU time [36]. GAUSSIAN DFT methods, by default, use a pruned 75 x 302 (radial x angular) grid which neglects points based on an atomic distance threshold. We found this grid to be too sparse

for the cases under study. Icosahedral molecules are not sampled well with the 302 point octahedral Lebedev angular grid, predicting for example, that icosahedral C_{60} is not the lowest energy isomer of buckminsterfullerene. These symmetry breaking problems are eliminated in calculations using the larger 75 x 590 point grid, which is utilized throughout this study in DFT methods.

Figure 2

Two views of four isomers of $\text{He}_2@C_{60}$
(D_{5d} , D_{3d} , D_{2d} , and D_{2h} symmetries)

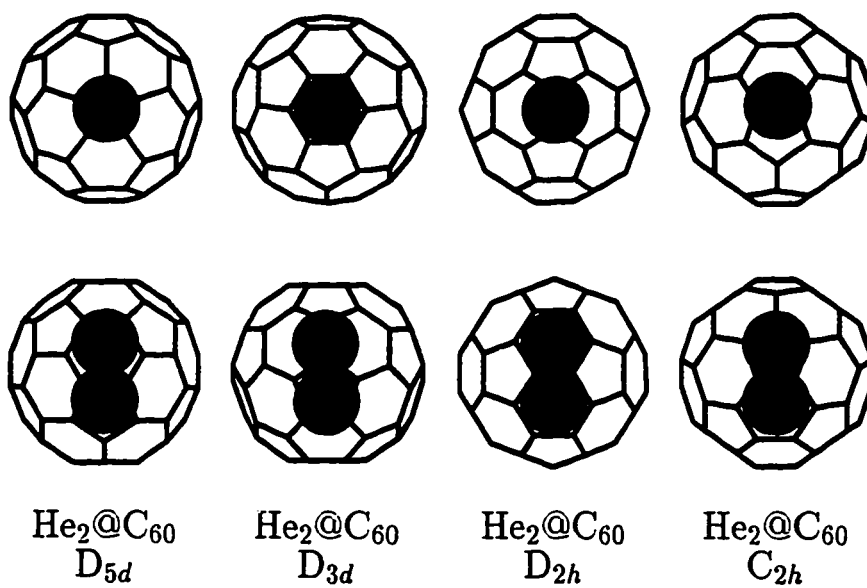
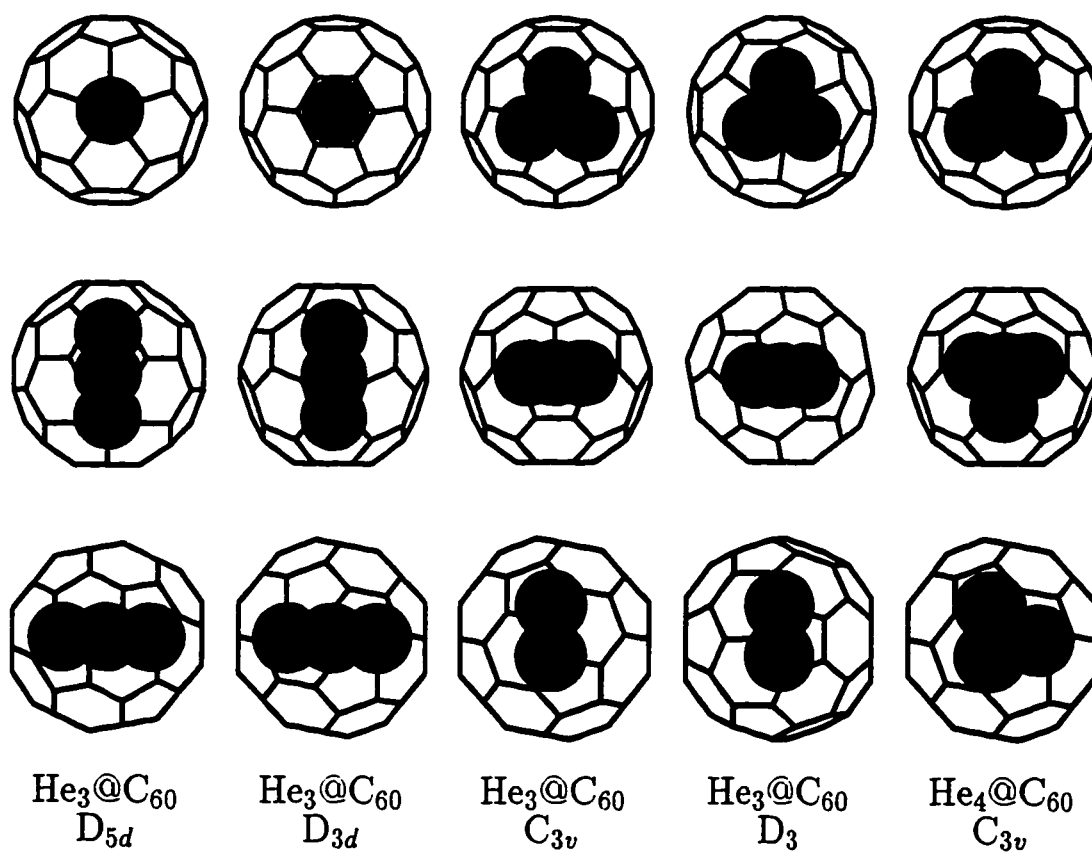


Figure 3
Three views of four isomers of $\text{He}_3@C_{60}$
(D_{5d} , D_{3d} , C_{3v} , and D_3 symmetries) and $\text{He}_4@C_{60}$ (C_{3v} symmetry)



Chapter 3

Results

Radii and the two symmetry distinct bond lengths of the single noble gas atom complexes of C_{60} are presented in Table 1. Optimized geometries of the icosahedral complexes are very similar to that of C_{60} at equilibrium, with radii within three thousandths of an Å of each other. For the smaller noble gas atom complexes, there is a slight shrinking of the radius of the fullerene, while for the larger noble gas atom complexes with C_{60} , the radius increases. Increasing the basis set size within level of theory decreases the radius and the 5-6 bonds, and increases the 6-6 bond lengths for these complexes.

Optimized radii of the multiple noble gas atom complexes are listed in Table 2. Average radii of all the multiple noble gas atom complexes are either equal to, or less than the radius of C_{60} at equilibrium, except for the linear $He_3@C_{60}$ complexes. Radii associated with the carbon atoms located equatorially to the axis on which the noble gas atoms lie decrease, while the radius of the carbon atoms nearest to the noble gas atom axis increase. The maximum radius of the fullerene is smaller when the noble gas atoms face open rings, rather than facing carbon-carbon bonds because of the increased noble gas-carbon atom interaction in the case of the latter. Also, the maximum radius is larger for complexes with noble gas atoms facing

pentagons than for those facing hexagons on the surface of the fullerene. Linear $\text{He}_3@C_{60}$ complexes are the most distorted of all the systems studied.

Binding energies of the single noble gas atom complexes are contained in Table 3. Energies calculated at different optimized geometries with the same level of theory are within 1 kcal/mol of each other. LSDA predicts that as the size of the noble gas atom inside C_{60} increases, the complex becomes more stable. B3LYP and MP2 predict destabilized energies, except for the $\text{Ne}@C_{60}$ complex.

CBEs are presented in Table 4. After BSSE is taken into account, LSDA still predicts that the complexes are binding, but to a lesser degree. $\text{Ne}@C_{60}$ is no longer binding at the B3LYP and MP2 levels of theory, but B3LYP predicts $\text{Ne}@C_{60}$ to be more stable than $\text{He}@C_{60}$, while the reverse is true for the MP2 calculations. B3LYP energies are on the average less than 1 kcal/mol from the MP2 values. Selected C_{60} strains are in Table 5. Only at the 3-21G/B3LYP//3-21G/LSDA level of theory does the geometry deformation create a noticeable energetic strain on the fullerene. In almost all of the other cases, the C_{60} strain is less than 0.05 kcal/mol.

Multiple noble gas atom complex energies are listed in Table 6. Only the $\text{Ne}_2@C_{60}$ complexes are predicted to be binding before BSSE corrections are made. After BSSE correction, the $\text{He}_2@C_{60}$ complexes are within 0.2 kcal/mol of each other, with the C_{2h} symmetry complex lower in energy, rather than the D_{5d} case, which has the least deformation. BSSE is very large for the $\text{Ne}_2@C_{60}$ complexes. Planar $\text{He}_3@C_{60}$ complexes are almost 30 kcal/mol lower in energy than their linear counterparts.

Results from the larger basis set calculations performed on representative group of complexes are presented in Table 7. BSSE is reduced to less than 20% of the total BE, compared to 40% or more, for the previous calculations. CBEs are within 1 kcal/mol, however, of the CBEs calculated with the smaller basis sets, so BSSE consideration is crucial to calculate accurate BEs for these systems, regardless of basis set size, at least up to 6-311G**. The CBE of the He₂@C₆₀ complex is predicted to be similar to that of Ar@C₆₀. Geometry strains of the fullerenes in the configuration of the noble gas atom complexes, compared to icosahedral C₆₀, display a trend of increased strain as the number of He atoms increased, which is not distinguished in the smaller basis set calculations. These strains remain less than 1 kcal/mol, however, even for the He₄@C₆₀ complex.

Table 1
 $X@C_{60}$ ($X = \text{He, Ne, Ar, Kr, and Xe}$)
 Optimized radii and bond lengths (\AA)

| | System | C_{60} Radius | 6-6 Bond | 5-6 Bond |
|---------------|--------------------|-----------------|----------|----------|
| 3-21G/LSDA | C_{60} | 3.538 | 1.389 | 1.450 |
| | $\text{He}@C_{60}$ | 3.537 | 1.388 | 1.450 |
| | $\text{Ne}@C_{60}$ | 3.537 | 1.388 | 1.449 |
| | $\text{Ar}@C_{60}$ | 3.536 | 1.388 | 1.449 |
| | $\text{Kr}@C_{60}$ | 3.537 | 1.388 | 1.449 |
| | $\text{Xe}@C_{60}$ | 3.538 | 1.389 | 1.450 |
| 6-31G**/LSDA | C_{60} | 3.529 | 1.392 | 1.442 |
| | $\text{He}@C_{60}$ | 3.529 | 1.392 | 1.442 |
| | $\text{Ne}@C_{60}$ | 3.528 | 1.392 | 1.441 |
| | $\text{Ar}@C_{60}$ | 3.529 | 1.392 | 1.442 |
| | $\text{Kr}@C_{60}$ | 3.528 | 1.392 | 1.442 |
| 3-21G/B3LYP | C_{60} | 3.555 | 1.391 | 1.459 |
| | $\text{He}@C_{60}$ | 3.555 | 1.391 | 1.459 |
| | $\text{Ne}@C_{60}$ | 3.554 | 1.390 | 1.459 |
| | $\text{Ar}@C_{60}$ | 3.556 | 1.391 | 1.459 |
| | $\text{Kr}@C_{60}$ | 3.557 | 1.391 | 1.460 |
| | $\text{Xe}@C_{60}$ | 3.559 | 1.392 | 1.461 |
| 6-31G**/B3LYP | C_{60} | 3.550 | 1.395 | 1.453 |
| | $\text{He}@C_{60}$ | 3.550 | 1.395 | 1.453 |
| | $\text{Ne}@C_{60}$ | 3.549 | 1.395 | 1.453 |
| | $\text{Ar}@C_{60}$ | 3.551 | 1.396 | 1.454 |
| | $\text{Kr}@C_{60}$ | 3.551 | 1.396 | 1.454 |

Table 2
 3-21G/LSDA $X_n@C_{60}$ ($X_n = He_2, Ne_2, He_3,$ and He_4)
 Optimized radii (Å)

| | Average C_{60} Radius | Minimum C_{60} Radius | Maximum C_{60} Radius |
|----------------------------|----------------------------|----------------------------|----------------------------|
| C_{60} (Ih) | 3.538 | | |
| $He_2@C_{60}$ (D_{5d}) | 3.537 | 3.536 | 3.543 |
| $He_2@C_{60}$ (D_{3d}) | 3.538 | 3.535 | 3.541 |
| $He_2@C_{60}$ (D_{2h}) | 3.537 | 3.535 | 3.546 |
| $He_2@C_{60}$ (C_{2h}) | 3.538 | 3.535 | 3.545 |
| $Ne_2@C_{60}$ (D_{5d}) | 3.537 | 3.534 | 3.550 |
| $Ne_2@C_{60}$ (D_{3d}) | 3.537 | 3.533 | 3.546 |
| $He_3@C_{60}$ (D_{5d}) | 3.541 | 3.524 | 3.594 |
| $He_3@C_{60}$ (D_{3d}) | 3.542 | 3.522 | 3.585 |
| $He_3@C_{60}$ (C_{3v}) | 3.538 | 3.534 | 3.553 |
| $He_3@C_{60}$ (D_3) | 3.538 | 3.533 | 3.552 |
| $He_4@C_{60}$ (C_{3v}) | 3.538 | 3.531 | 3.557 |

Table 3
 $X@C_{60}$ (X = He, Ne, Ar, Kr, and Xe)
 Binding energies (kcal/mol)

| | He @ C ₆₀ | Ne @ C ₆₀ | Ar @ C ₆₀ | Kr @ C ₆₀ | Xe @ C ₆₀ |
|----------------------------|----------------------------|----------------------------|----------------------------|----------------------------|----------------------------|
| 3-21G/LSDA//3-21G/LSDA | -1.1 | -2.6 | -16.6 | -18.3 | -21.1 |
| 6-31G**/LSDA/3-21G/LSDA | -2.1 | -5.9 | -11.3 | -24.6 | |
| 6-31G**/LSDA//6-31G**/LSDA | -2.1 | -5.9 | -11.1 | -24.6 | |
| 3-21G/B3LYP//3-21G/LSDA | 0.8 | -1.2 | 3.7 | 8.6 | 20.8 |
| 6-31G**/B3LYP//3-21G/LSDA | 0.9 | -2.3 | 6.9 | 1.8 | |
| 6-31G**/B3LYP//3-21G/B3LYP | 0.6 | -2.6 | 6.0 | 1.1 | |
| 3-21G/MP2//3-21G/B3LYP | 0.1 | -0.7 | 3.9 | 10.5 | 25.0 |
| 6-31G**/MP2//3-21G/B3LYP | 0.2 | -1.2 | 7.5 | 4.8 | |
| 6-31G**/MP2//6-31G**/B3LYP | 0.1 | -1.0 | 8.0 | 4.7 | |

Table 4
 X@C₆₀ (X = He, Ne, Ar, Kr, and Xe)
 BSSE corrected binding energies (kcal/mol)

| | He @ C ₆₀ | Ne @ C ₆₀ | Ar @ C ₆₀ | Kr @ C ₆₀ | Xe @ C ₆₀ |
|---|----------------------------|----------------------------|----------------------------|----------------------------|----------------------------|
| 3-21G/LSDA//3-21G/LSDA | -0.3 | 0.0 | -10.6 | -8.6 | -9.2 |
| 6-31G**/LSDA/3-21G/LSDA | -1.3 | -2.2 | -9.0 | -10.1 | |
| 6-31G**/LSDA//6-31G**/LSDA | -1.3 | -2.2 | -8.8 | -10.0 | |
| 3-21G/B3LYP//3-21G/B3LYP | 1.3 | 1.0 | 8.7 | 17.5 | 31.3 |
| 6-31G**/B3LYP//3-21G/B3LYP | 1.2 | 0.7 | 8.2 | 14.8 | |
| 6-31G**/B3LYP//6-31G**/B3LYP ^c | 1.4 | 0.9 | 8.4 | 15.0 | |
| 3-21G/MP2//3-21G/B3LYP | 0.6 | 1.1 | 8.3 | 18.7 | 36.3 |
| 6-31G**/MP2//3-21G/B3LYP | 0.6 | 1.1 | 8.7 | 17.2 | |
| 6-31G**/MP2//6-31G**/B3LYP ^c | 0.6 | 1.3 | 9.2 | 17.1 | |

^c BSSE taken from 6-31G**//3-21G

Table 5
X@C₆₀ (X = He, Ne, Ar, Kr, and Xe)
C₆₀ strains (kcal/mol)

| | He @ C ₆₀ | Ne @ C ₆₀ | Ar @ C ₆₀ | Kr @ C ₆₀ | Xe @ C ₆₀ |
|---------------------------|----------------------------|----------------------------|----------------------------|----------------------------|----------------------------|
| 3-21G/LSDA//3-21G/LSDA | 0.0 | 0.0 | 0.0 | 0.0 | 0.0 |
| 6-31G**/B3LYP//3-21G/LSDA | 0.1 | 0.3 | 0.5 | 0.4 | 0.1 |
| 3-21G/B3LYP//3-21G/B3LYP | 0.0 | 0.0 | 0.0 | 0.0 | 0.1 |

Table 6
 3-21G/B3LYP//3-21G/LSDA $X_n@C_{60}$ ($X_n = He_2, Ne_2, He_3,$ and He_4)
 Binding energies, BSSE corrected BEs, and C_{60} strains (kcal/mol)

| | Binding Energy | Corrected BE | C_{60} Strain |
|----------------------------|----------------|--------------|-----------------|
| $He_2@C_{60}$ (D_{5d}) | 4.3 | 8.6 | 0.3 |
| $He_2@C_{60}$ (D_{3d}) | 4.2 | 8.5 | 0.2 |
| $He_2@C_{60}$ (D_{2h}) | 4.1 | 8.5 | 0.3 |
| $He_2@C_{60}$ (C_{2h}) | 4.1 | 8.4 | 0.2 |
| $Ne_2@C_{60}$ (D_{5d}) | -2.7 | 27.0 | 0.5 |
| $Ne_2@C_{60}$ (D_{3d}) | -2.8 | 27.0 | 0.5 |
| $He_3@C_{60}$ (D_{5d}) | 38.8 | 47.1 | 1.4 |
| $He_3@C_{60}$ (D_{3d}) | 37.6 | 45.6 | 1.1 |
| $He_3@C_{60}$ (C_{3v}) | 10.3 | 17.4 | 0.2 |
| $He_3@C_{60}$ (D_3) | 10.2 | 17.4 | 0.3 |
| $He_4@C_{60}$ (C_{3v}) | 18.3 | 28.3 | 0.2 |

Table 7
6-311G**/B3LYP//3-21G/B3LYP $X_n@C_{60}$ ($X_n = He_2, Ne_2, He_3,$ and He_4)
Binding energies, BSSE corrected BEs, and C_{60} strains (kcal/mol)

| | Binding Energy | Corrected BE | C_{60} Strain |
|---|----------------|--------------|-----------------|
| He@ C_{60} (Ih) | 1.0 | 1.3 | 0.0 |
| Ne@ C_{60} (Ih) | -2.7 | 1.1 | -0.1 |
| Ar@ C_{60} (Ih) | 5.8 | 7.2 | 0.1 |
| Kr@ C_{60} (Ih) | 11.9 | 13.8 | 0.3 |
| He ₂ @ C_{60} (D_{5d}) | 6.0 | 7.2 | 0.2 |
| Ne ₂ @ C_{60} (D_{5d}) | 14.2 | 24.8 | 0.4 |
| He ₃ @ C_{60} (D_3) | 15.1 | 17.0 | 0.4 |
| He ₄ @ C_{60} (C_{3v}) | 26.6 | 29.1 | 0.8 |

Chapter 4

Conclusions

High level density functional and perturbation theory calculations are performed on several noble gas atom complexes with C_{60} . Fully optimized radii of the icosahedral complexes, and the average radii of the multiple noble gas atom complexes differ from that of C_{60} at equilibrium by only a few thousandths of an Å. The B3LYP and MP2 interaction energies for the smaller noble gas atom complexes of He and Ne are consistently predicted by both methods to be slightly repulsive, about 1 kcal/mol. It is interesting to note that B3LYP and MP2 predictions are very similar for the problem under consideration. These energies are much more repulsive for the other noble gas atom complexes, around 7 and 14 kcal/mol for $Ar@C_{60}$ and $Kr@C_{60}$, and from 7 to 30 kcal/mol for the $He_2@C_{60}$ and $He_4@C_{60}$ complexes. As expected, C_{60} is resilient to deformation in all cases studied, with strains of the fullerene in the geometry of the complex less than 0.5 kcal/mol for the single noble gas atom complexes, and less than 1 kcal/mol for all multiple noble gas atom complexes studied with realistic geometries.

With the possibility of over 100% incorporation of noble gas atoms into C_{60} , multiple noble gas atom complexes may be formed in the future. Calculations performed here predict that if C_{60} will be able to withstand multiple noble gas atom insertion, $He_2@C_{60}$ will be as stable as the currently created $Ar@C_{60}$ complex. The

resilient C_{60} cage is a perfect nano-sized container for atoms and small molecules. If this container concept is carried over to larger applications, the effects of endohedral atoms and molecules on larger sized fullerenes will require future attention.

References

- [1] H.W. Kroto, J.R. Heath, S.C. O'Brien, R.F. Curl, R.E. Smalley, *Nature*, 318 (1985) 162.
- [2] W. Kratchmer, L.D. Lamb, K. Fostiropoulos, D.R. Huffman, *Nature*, 347 (1990) 354.
- [3] D.L. Strout, G.E. Scuseria, *J. Phys. Chem.*, 100, (1996) 6492.
- [4] K. Hedberg, L. Hedberg, D.S. Bethune, C.A. Brown, H.C. Dorn, R.D. Johnson, M. de Vries, *Science*, 254 (1991) 410.
- [5] J. Cioslowski, *Electronic Structure Calculations on Fullerenes and Their Derivatives*, Oxford University Press, New York, 1995.
- [6] J.A. Dean, ed., *Lange's Handbook of Chemistry*, Mc-Graw Hill Book Co., NY, 1979.
- [7] M. Saunders, H.A. Jimenez-Vazquez, R.J. Cross, R.J. Poreda, *Science*, 259 (1993) 1428.
- [8] R.J. Poreda, K.A. Farley, *Earth Planet. Sci. Lett.*, 113 (1992) 97.
- [9] M. Saunders, H.A. Jimenez-Vazquez, R.J. Cross, S. Mroczkowski M.L. Gross, D.E. Giblin, R.J. Pedora, *J. Am. Chem. Soc.*, 116 (1994) 2193.
- [10] M. Saunders, R.J. Cross, H.A. Jimenez-Vazquez, R. Shimshi, A. Khong, *Science*, 271 (1996) 1693.
- [11] R. Shimshi, A. Khong, H.A. Jimenez-Vazquez, R.J. Cross, M. Saunders, *Tetrahedron*, 52 (1996) 5143.
- [12] Z. Xu, and J. Yan, *Int. J. Quantum Chem.*, 53 (1995) 287.
- [13] 6-31G**/B3LYP level of theory. Benzene and C₂₄H₁₂ both had C_{6v} symmetry TS structures. For a summary of benzene TS energies, see ref [17].
- [14] T. Weiske, D.K. Bohme, J. Hrusak, W. Kratschmer, H. Schwarz, *Angew. Chem. Int. Ed. Engl.*, 30 (1991) 884.
- [15] K.A. Caldwell, D.E. Giblin, M.L. Gross, *J. Am. Chem. Soc.*, 114 (1992) 3743.

- [16] R.L. Murry, G.E. Scuseria, *Science*, 263 (1994) 791.
- [17] S. Patchkovskii, W. Thiel, *J. Am. Chem. Soc.*, 118 (1996) 7164.
- [18] J.R. Heath, S.C. O'Brien, Q. Zhang, Y. Liu, R.F. Curl, H.W. Kroto, F.K. Tittel, R.E. Smalley, *J. Am. Chem. Soc.*, 107 (1985) 7779.
- [19] F.D. Weiss, J.L. Elkind, S.C. O'Brien, R.F. Curl, R.E. Smalley, *J. Am. Chem. Soc.*, 110 (1988) 4464.
- [20] H. Shinohara, H. Sato, Y. Saito, M. Okhohchi, Y. Ando, *J. Phys. Chem.*, 96 (1992) 3571.
- [21] H. Shinohara, H. Sato, M. Okhohchi, Y. Ando, T. Shinda, T. Kato, Y. Saito, *Nature*, 357 (1992) 52.
- [22] J.C. Hummelen, M. Prato, F. Wudl, *J. Am. Chem. Soc.*, 117 (1995) 7003.
- [23] M.J. Arce, A.L. Viado, Y.Z. An, S.I. Khan, Y. Rubin, *J. Am. Chem. Soc.*, 118 (1996) 3775.
- [24] T. P. Thrash, D. W. Cagle, M. Alford, G. J. Ehrhardt, J. C. Iattimer, L. J. Wilson, submitted to *Nature*.
- [25] K. Kobayashi, S. Nagase, T. Akasaka, *Chem. Phys. Lett.* 261 (1996) 502.
- [26] A.B. Smith III, R.M. Strongin, L. Brard, W.J. Romanow, M. Saunders, H.A. Jimenez-Vazquez, R.J. Cross, *Tetrahedron Lett.*, 1994 (1994) 3689.
- [27] J. Cioslowski, *J. Chem. Soc.*, 113 (1991) 4139.
- [28] J. Cioslowski, E.D. Fleishmann, *J. Chem. Phys.*, 94 (1991) 3730.
- [29] R.G. Parr, W. Yang, *Density-Functional Theory of Atoms and Molecules*, Oxford University Press, New York, 1989.
- [30] A.D. Becke, *J. Chem. Phys.*, 98 (1993) 5648.
- [31] A.D. Becke, *Phys. Rev. A*, 33 (1986) 2786.
- [32] J. Baker, M. Muir, J. Andzelm, *J. Chem. Phys.*, 102 (1995) 2063.
- [33] J.A. Pople, R. Seeger, R. Krishnan, *Int. J. Quant. Chem. Symp.*, 11 (1977) 149.
- [34] S.F. Boys, F. Bernardi, *Mol. Phys.*, 19 (1970) 553.
- [35] GAUSSIAN 95, Development Version (Revision D.4), M.J. Frisch, G.W. Trucks, H.B. Schlegel, G.E. Scuseria, M.A. Robb, J.R. Cheeseman, M.C.

Strain, J.C. Burant, R.E. Stratmann, G.A. Petersson, J.A. Montgomery, V.G. Zakrzewski, T. Keith, K. Raghavachari, M.A. Al-Laham, J.V. Ortiz, J.B. Foresman, J. Cioslowski, B.B. Stefanov, A. Nanayakkara, M. Challacombe, C.Y. Peng, P.Y. Ayala, W. Chen, M.W. Wong, J.L. Andres, E.S. Replogle, R. Gomperts, R.L. Martin, D.J. Fox, J.S. Binkley, D.J. Defrees, J. Baker, J.P. Stewart, C. Gonzalez, M. Head-Gordon, P.M.W. Gill, B.G. Johnson, and J.A. Pople, Gaussian, Inc., Pittsburgh PA, 1996.

- [36] R.E. Stratmann, G.E. Scuseria, M.J. Frisch, *Chem. Phys. Lett.*, 257 (1996) 213.